



## Research article

# Repurposing of Food and Drug Administration (FDA) approved library to identify a potential inhibitor of *trypanothione synthetase* for developing an antileishmanial agent

Divya Vemula<sup>1</sup>, Shreelekha Mohanty<sup>1</sup>, Vasundhra Bhandari<sup>\*</sup>

Department of Pharmacoinformatics, National Institute of Pharmaceutical Education and Research, Hyderabad, India

## ARTICLE INFO

## Keywords:

Homology modeling  
Leishmaniasis  
Molecular dynamics simulation  
Trypanothione synthetase  
Virtual screening

## ABSTRACT

Leishmaniasis is one of the top 10 neglected tropical diseases. Globally, it impacts more than 12 million individuals. In light of the absence of a safer, affordable treatment for the Leishmaniasis, along with therapeutic failures and drug resistance, novel therapeutic strategies are necessary to discover new drugs. Treatment would benefit by concentrating on the precise targets that are crucial for the parasite to survive. A target that aids in the organism's survival under oxidative stress is trypanothione synthetase (TyS), which is a component of the trypanothione pathway in *Leishmania* spp. To find potential TyS inhibitors for the purpose of discovering novel anti-leishmanial drugs, we used a virtual screening strategy. Using the Glide module of Schrodinger-suite 2023, an FDA-approved library containing 2000 drugs from the ZINC-15 database was screened against the TyS. Dostinex, raloxifene, and formoterol showed good docking scores of  $-10.568$  kcal/mol,  $-10.446$  kcal/mol, and  $-56.21$  kcal/mol, as well as good binding energies of  $-70.41$  kcal/mol,  $-56.21$  kcal/mol, and  $-64.15$  kcal/mol respectively. The stability of the ligand-protein complexes was assessed further with the help of Desmond to execute a 100-ns molecular dynamics simulation. The Prime module was utilised to perform post-MM/GBSA analysis on these three molecules along with the toxicity profiling using Protox II web server. This study suggests that dostinex, formoterol, and raloxifene may act as effective inhibitors of the TyS receptor which could be used as novel antileishmanial agents for the therapeutic applications. Thorough preclinical studies are necessary to confirm the identified compounds chemotherapeutic qualities.

## 1. Introduction

Leishmaniasis is a tropical illness exclusively found in South and Central America, Northern Africa, and Asia. This infection is caused by the digenetic and intracellular protozoa *Leishmania* spp. (approximately 21 pathogenic species), with sandfly (*Phlebotomus* or *Lutzomyia* spp.) serving as the primary transmission vector [1]. There are three main types of leishmaniasis, cutaneous, mucocutaneous, and visceral. The most severe form of leishmaniasis among the three is visceral leishmaniasis (VL, or Kala-azar), a fatal infection of the liver, spleen, and bone marrow. The common symptoms of VL include fever, splenomegaly, hypergammaglobulinemia,

<sup>\*</sup> Corresponding author. Department of Pharmacoinformatics National Institute of Pharmaceutical Education and Research (NIPER), Balanagar, Hyderabad, Telangana, 500037, India.

E-mail addresses: [vasundhra23@gmail.com](mailto:vasundhra23@gmail.com), [vasundhra.b@niperhyd.ac.in](mailto:vasundhra.b@niperhyd.ac.in) (V. Bhandari).

<sup>1</sup> Authors contributed equally.

<https://doi.org/10.1016/j.heliyon.2024.e27602>

Received 2 August 2023; Received in revised form 2 March 2024; Accepted 4 March 2024

Available online 11 March 2024

2405-8440/© 2024 Published by Elsevier Ltd.

This is an open access article under the CC BY-NC-ND license

(<http://creativecommons.org/licenses/by-nc-nd/4.0/>).

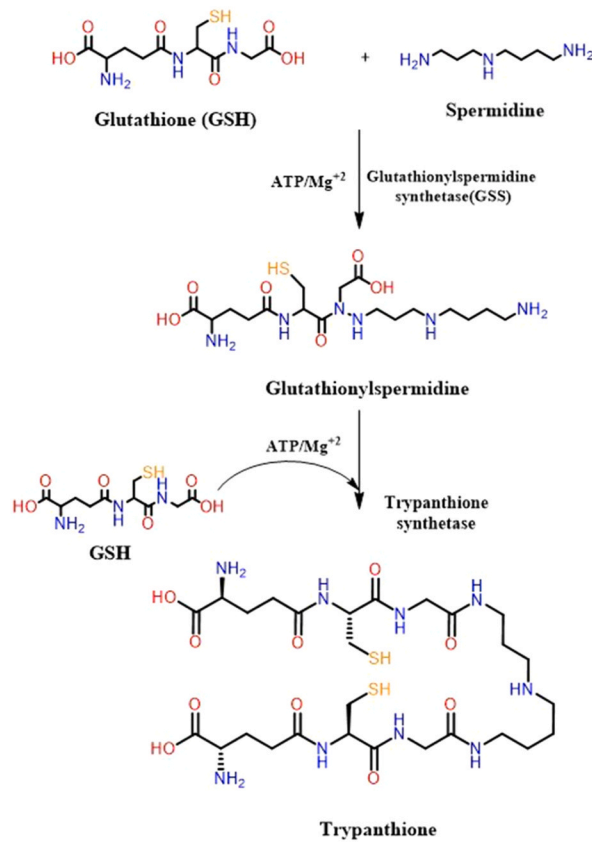


Fig. 1. Biosynthesis of Trypanthione in *Leishmania donovani* from Glutathione and Spermidine molecule by the enzyme Trypanthione synthetase.

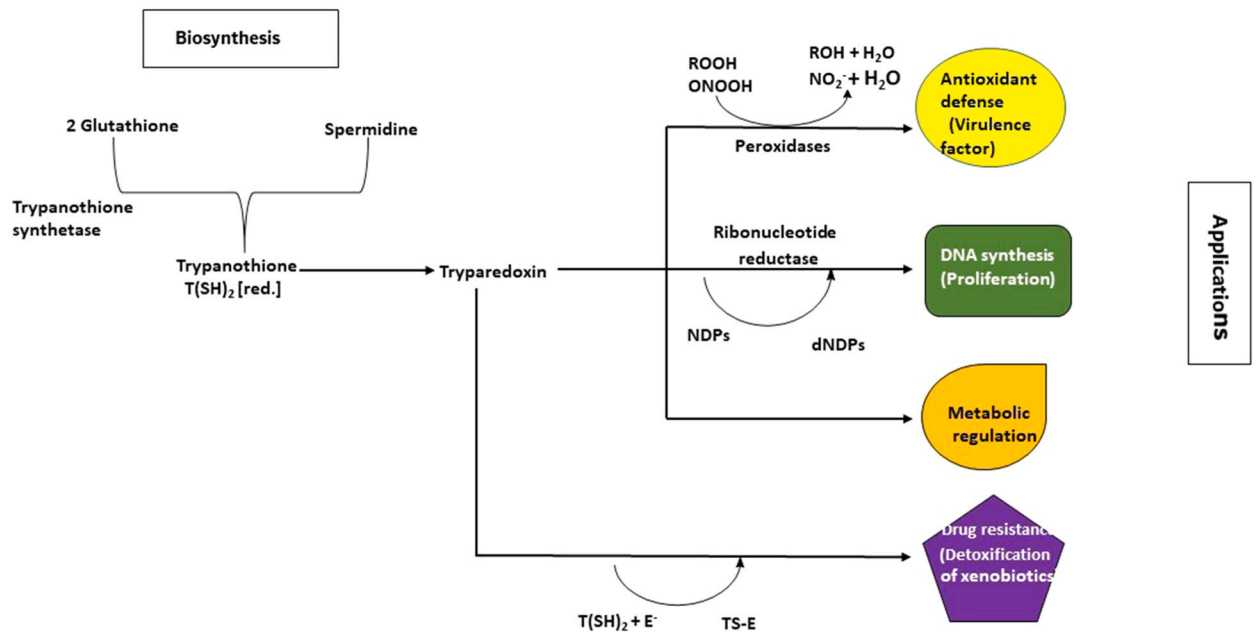


Fig. 2. Various functions of Trypanthione in *Leishmania donovani*.

and pancytopenia, which could be fatal if left untreated [2]. An estimated 50000 to 90000 new cases of VL occur worldwide annually [<https://www.who.int/news-room/fact-sheets/detail/leishmaniasis>]. It remains one of the top parasitic diseases with outbreak and mortality potential. The etiological agent of VL is *L. donovani* and *L. infantum* [3]. Only chemotherapeutic agents are available to control VL due to the absence of vaccine [4]. Amphotericin B is considered the drug of choice for VL. Alternatives drugs also used in VL are miltefosine, paromomycin, and pentavalent antimonials [5]. But these drugs are ineffective because of the emergence of resistance, followed by several side effects, including high toxicity, teratogenic effect, longer half-life, lack of efficacy, and high cost making drugs vulnerable to the rapid development of drug resistance [6]. So, for the treatment of leishmaniasis, finding novel drugs is crucial due to the constraints mentioned above. Additionally, to the usual issues with activity and specificity, the drugs' ability to kill parasites depends on their ability to pass through three different cell membranes: the host cell plasma membrane, the phagolysosome membrane, and the parasite plasma membrane. So, there is an immediate need to discover novel, cost-effective, and highly potent anti-leishmanial drugs. Good prospects for drug discovery include focusing on specific cellular functions and metabolic pathways different from those of other eukaryotes [7]. The *Leishmania* parasite's growth and proliferation are regulated by various metabolic pathways like sterol biosynthesis, purine salvage, glycosyl phosphatidyl inositol (GPI) biosynthesis, folate biosynthesis, hypusine, and the trypanothione pathway. Therefore, these pathways are important therapeutic targets for treating *Leishmania* infection due to their crucial role [8]. Among these above-mentioned pathways, the trypanothione pathway is an essential metabolic pathway for parasitic survival. One of the unique metabolic pathways distinctive to *Leishmania* and other trypanosomatids is the synthesis of trypanothione, which doesn't exist in other eukaryotes. It aids in the regulation of *Leishmania*'s oxidative stress. The metabolic byproduct of this process is trypanothione T(SH)<sub>2</sub>. The aforementioned peptide-amine conjugate is synthesised in two stages through the assistance of trypanothione synthetase (TyS), two ATP molecules, one Glutathione (GSH) molecule (a tripeptide generated by the enzyme glutamyl-cysteine synthetase (-GSH) and utilised in the body's reaction to oxidative stress), and one spermidine (Spd) molecule (produced via the polyamine pathway and involved in cellular differentiation and proliferation) [9] (Fig. 1). T(SH)<sub>2</sub> is essential for several parasite cellular functions, such as DNA synthesis, drug resistance, defence against chemical and oxidative stress, and intracellular thiol redox equilibrium management. Additionally, it keeps polyamine levels stable, which is necessary for cellular differentiation and proliferation (Fig. 2). The role of TyS in trypanothione pathway was demonstrated by dsRNA interference knock-down in *Trypanosoma* species, which eventually led to a decrease in T(SH)<sub>2</sub> and glutathione-spermidine (GSp) levels despite an increase in GSH levels. This, in turn, caused a concurrent growth arrest, impaired antioxidant capacity, decreased infectivity, and ultimately the death of parasitic cells. This finding led to the understanding that the parasite's defence mechanism against oxidative stress is severely disrupted by the decrease of TyS. Since the TyS gene is a part of the upstream thiol metabolic cascade, GSH cannot take the place of T(SH)<sub>2</sub> activities. Different trypanosomatid taxa have different processes for producing T(SH)<sub>2</sub>. Like *L. major* and *L. braziliensis*, *L. donovani* and *L. amazonens* is also entirely rely on the TyS enzyme for T(SH)<sub>2</sub> production. This single-copy gene encodes a protein with two distinct functions: synthetase activity located in the middle domain (20–25 amino acids) and amidase activity located at the protein's N and C termini.

The amidase activity reversibly converts T(SH)<sub>2</sub> back into GSH and Spd while the synthetase activity uses a catalytic method to create T(SH)<sub>2</sub>. T(SH)<sub>2</sub> contributes to resistance development, intracellular thiol redox balance maintenance, and DNA synthesis [10]. Targeting this enzyme provides target specificity since TyS is absent in humans. In *Leishmania*, the three essential metabolites—trypanothione, glutathione-spermidine, and spermidine—are regulated by the enzyme TyS, whose blockage causes the death of the parasite [11]. Thus, it may be advantageous to target the TyS enzyme in order to find new, promising medications to treat leishmaniasis. The objective of the current study is to identify trypanothione synthetase inhibitors using virtual screening and molecular dynamic simulation approaches to assess new potential inhibitors of TyS enzyme. The development of medications for a number of disorders, including drug repositioning, has been considerably aided by *in silico* techniques, which have also shortened the cost and time of discovery. There are numerous computational methods available for repurposing drugs [12]. The aim of the current study is to identify novel, potential TyS inhibitors using a successful computational strategy i.e., structure based virtual screening [13] and to analyze the stabilities of hit molecules using molecular dynamic simulation along with the analysis of toxicity profiles in order to find out the existing drugs that can be repurposed for the treatment of leishmaniasis.

## 2. Material and methods

### 2.1. Conservation of TyS

The NCBI-BLAST tool [14] was utilised to establish the conservation of the TyS protein sequence among different *Leishmania* species. This tool locates local similarity regions between sequences by utilising the Smith-Waterman algorithm and the BLOSUM62 scoring matrix. Later, in order to identify the regions of similarity that indicate the structural, functional, and evolutionary relationship between the two sequences, a pairwise sequence alignment of the TyS protein of the top hit, or *L. major*, with the TyS protein of *L. donovani* was conducted using Clustal Omega [15]. As its primary alignment engine, Clustal Omega employs the HHalign algorithm with default settings.

### 2.2. Homology modeling

The 3D structure of the Tys protein of *L. donovani* is not available in the Protein Data Bank (PDB) database. The BLAST similarity search was performed to find the sequence similar to the TyS protein of *L. donovani* for homology modeling. The Tys sequence of *L. major* (Uniprot ID-G5D5D5) was retrieved from the Uniprot database. Using the Schrodinger suite, the homology modeling of the

protein TyS was carried out [16]. The generated protein model was validated using the Ramachandran plot and the Schrodinger suite protein reliability report to confirm the predicted model's stereo-chemical stability. These parameters included the percentage of residues lying in disallowed and allowed regions, the number of glycine and proline residues, the orientation of dihedral angles including phi and psi angle, and backbone conformation.

### 2.3. Protein preparation

The protein model structure was built by the "protein preparation wizard" of Schrodinger-suite by removing water molecules. After that, the hydrogen atoms were added, and the bond order was allocated. Finally, a restrained minimization of the model protein structure was built by using the OPLS4 force field [17]. Using the sitemap module of Schrodinger, the active site of the model protein was identified based on the Site-Score and D score (druggability score). After that, a receptor grid was generated to define the target protein's active site for docking using Receptor grid generation panel of Schrodinger suite. The protein atoms' van der Waal radii were scaled by 1.0, and the polarity charge threshold was 0.25. The receptor grid box was also created in each direction ( $x = 27 \text{ \AA}$ ,  $y = 27 \text{ \AA}$ , and  $z = 27 \text{ \AA}$ ), and it was positioned in the middle of the cognate ligands with space for any ligand to fit inside the binding pocket [18]. Following grid generation, the dock main was  $27 \text{ \AA}$  in each dimension ( $x$ ,  $y$ , and  $z$ ).

### 2.4. Ligand source and virtual screening

A total of 2000 small molecules were obtained in Structure Data Format (SDF) from FDA-approved drugs of the ZINC15 database. The "virtual screening workflow" (VSW) panel of Schrodinger was used to screen the compound against the TyS protein. Initially the ligands were imported into the VSW panel, the van der Waals scaling factor was set to 0.85 and 0.15, and the partial charges limit value was set at  $-10.0 \text{ kcal/mol}$  for non-polar ligand atoms. The total compound library was screened against TyS receptor by running an entire series of tasks through the VSW. The process entails ligand preparation using LigPrep in order to assign correct bond ordering and generate a three-dimensional geometry, ligand preparation was carried out on the downloaded SDF files. This was completed in Maestro Schrodinger Suite 2023 with the Ligprep force field and OPLS4. Furthermore, ionisation states were produced at  $\text{pH } 7.0 \pm 2.0$  using Epik 2.2. For each ligand, we produced 32 potential stereoisomers., filtering on pharmacokinetic characteristics with the Qikprop or other structural parameters using ligfilter, and Glide docking at the three accuracy levels, High throughput virtual screening (HTVS), standard precision (SP), and extra precision (XP) [19] using OPLS4 force field and Emodel1 scoring function. The ligands were given complete flexibility and glide's HTVS scoring functions as well as SP were employed. On the ligand-receptor complexes that were produced, a post-docking minimization was performed, which decreased the ligands' initial collected poses. Further docking of the SP resulting compounds was done with more accuracy and computational intensity using the XP mode. There was no flexibility, relaxation, or minimization in the setup. The process obtained the lead ligand-receptor complexes based on the glide energy and XP glide rescoring. The receptor-ligand interactions were visualized using 2D viewer of Schrodinger [20].

### 2.5. Prime MM/GBSA/free energy calculation

To predict the binding free energy of the targeted protein-ligand docked complex, the prime MM/GBSA (molecular mechanics and generalized born surface area) module of Schrodinger-suite 2022 was used. The larger negative MM/GBSA value indicates that the ligand has a strong binding affinity with the target protein. Prime MM/GBSA process constitutes OPLS molecular mechanics force field, a surface-generalized Born (SGB) implicit solvation model, and a nonpolar solvent. The binding free energy ( $\Delta G_{\text{bind}}$ ) was calculated by using the following equation [21].

$$\Delta G_{\text{bind}} = G_{\text{complex}} - (G_{\text{protein}} + G_{\text{ligand}})$$

The  $G_{\text{complex}}$  indicates complex energy,  $G_{\text{protein}}$  indicates receptor energy, and  $G_{\text{ligand}}$  indicates the unbound ligand energy.

### 2.6. Molecular dynamic simulation and post MM/GBSA

The hits obtained after the virtual screening were further subjected to molecular dynamic simulation. To examine the conformational stability of the protein-ligand complex in the solvated model system embedded with ordered water molecules (ordered water molecules may be involved in protein binding sites and influence protein-ligand binding by bridging protein-ligand interactions and can make significant contributions to the binding affinity) MD simulation studies were carried out for 100 ns using Desmond module. It supports all the standard algorithms for quick and precise MD simulations. First, the complexes were solvated with the single point charge (SPC) water model, and then the ions were neutralized by counter ion  $\text{Na}^+$  and  $\text{Cl}^-$  to prepare them for simulation. The MD simulation was carried out using NPT (constant Pressure temperature) ensemble with constant temperature and constant pressure ensemble at constant volume with 300 K temperature and 1atm pressure. Throughout the simulation period, parameters like root mean square deviation (RMSD), root mean square fluctuation (RMSF), hydrogen bond interaction, the radius of gyration ( $R_g$ ), molecular surface area (MolSA), and solvent-accessible surface area (SASA) were analyzed to predict the structural and dynamic properties of the protein-ligand complexes [22]. Additionally, using the prime MM/GBSA module in Schrodinger, the post-MM/GBSA analysis was done to determine the binding energy.

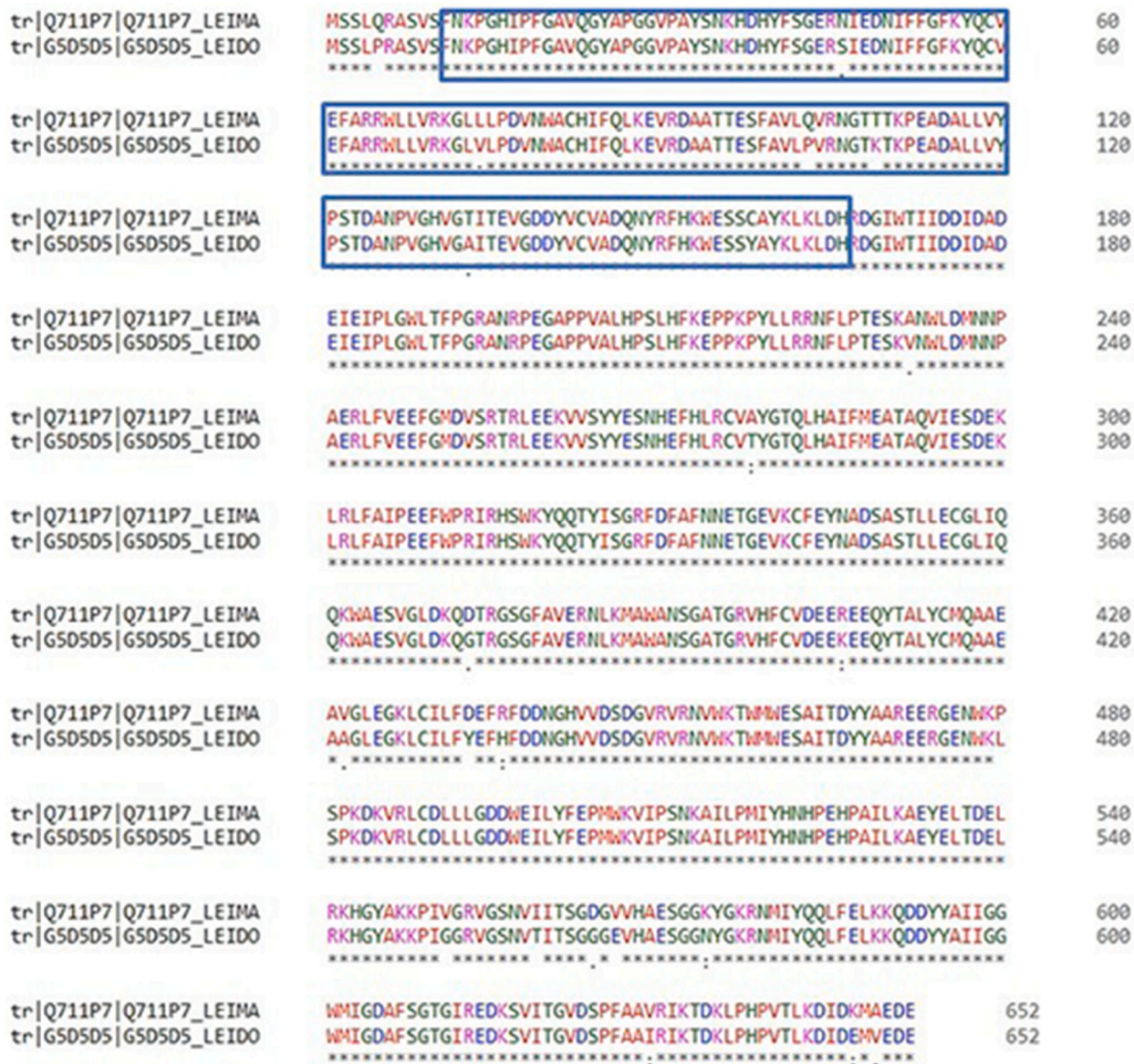
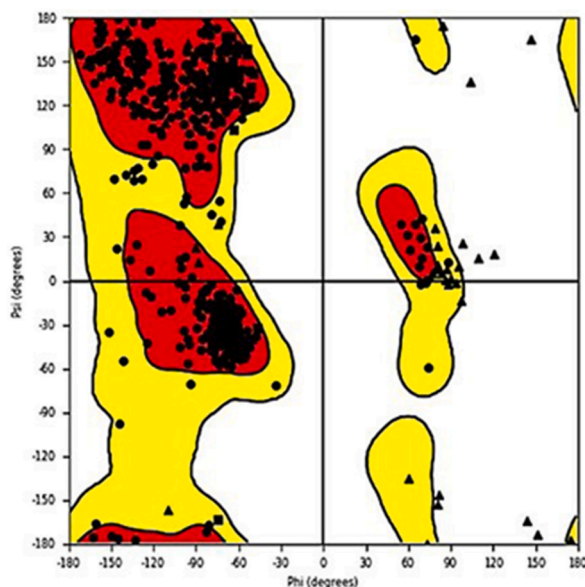


Fig. 3. Pairwise Sequence alignment of TyS of Leishmania donovani and Leishmania major by using Clustal omega. Showing the sequence similarity of 96.47%.

### 2.7. Toxicity prediction

For toxicity prediction of the top 3 compounds, the ProTox-II web server was used. The compound's name or the SMILES (Simplified Molecular-Input Line-Entry System) string of the compound was entered to forecast probable toxicities related to its chemical structure [23]. After that, organ toxicity and toxicity endpoints like carcinogenicity, immunotoxicity, mutagenicity, cytotoxicity, and Tox21 Nuclear receptor signalling pathways, followed by Tox21 stress response pathways, were selected. The predictions are made quickly for both the acute toxicity and toxicity targets. The results page contains the predicted median fatal dosage (LD50) in mg/kg weight, the toxicity class, the prediction accuracy, the average similarity, and the three dangerous substances from the dataset that are most similar to each other and have known rodent oral toxicity values. Toxicity classes are classified into five classes according to the globally harmonized system of classification (GSH). According to GSH, the compounds are said to be class-1 if they have LD50 values less than or equal to 5 mg. Compounds are said to be class-2 if their LD50 value lies between 5 and 50 mg. Class-1 and class-2 drugs are fatal. Compounds are said to be in class-3 if they have lethal doses between 50 and 300 mg, and these are toxic if swallowed. Class-4 and class-5 compounds are not that much toxic as their lethal dose range is high(300–5000 mg). Class-6 compounds are not toxic as their lethal dose is greater than 5000 mg [24].



**Fig. 4.** Ramachandran plot of modelled TyS protein. Dots in the plot represent amino acid residues. Red colour represents the allowed region, yellow colour represents the favoured region, and white colour represents the disallowed region in the plot respectively. In this plot, most of the amino acids are present in the allowed region (>90%).

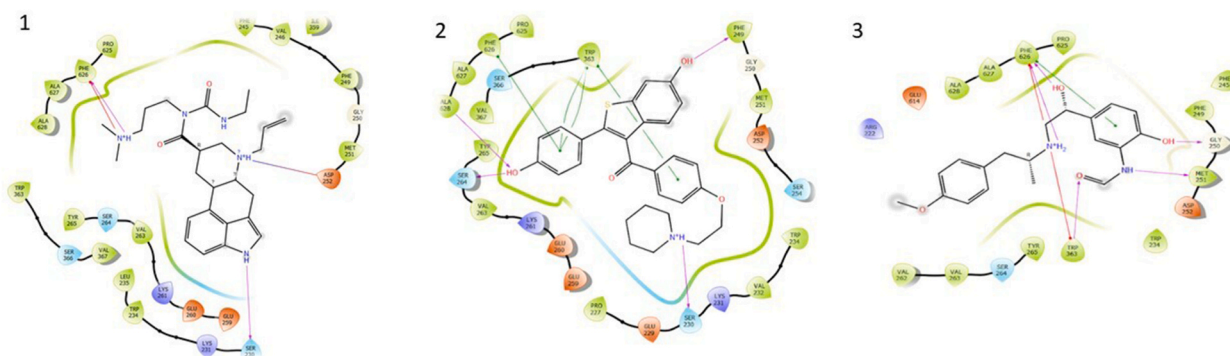


**Fig. 5.** Binding affinity and amino acid interactions of top three compounds with TyS protein. The purple, green and red arrows represent hydrogen bonding, Pi-Pi stacking and Pi-cation interactions between protein and ligands respectively, (a) Dostinex [-11.927 kcal/mol], (b) Raloxifene [-10.568 kcal/mol] and (c) Formoterol [-10.446 kcal/mol].

### 3. Result & discussion

#### 3.1. Conservation of TyS

TyS protein conservation was determined using BLAST of all sequences in the UniProt database. It was found to be conserved in most *Leishmania* species including *L. major*, *L. mexicana*, *L. infantum*, *L. tarentolae* etc but absent in *Homo sapiens*. *L. donovani* TyS protein (reference sequence) was used for the BLAST search, and the similarity between the sequences was calculated. As a result of the TyS sequence alignment, it produced 101 hits with percentage identities ranging from 100% to 38%. Pairwise sequence alignment of TyS proteins from *L. major* and *L. donovani* revealed the highest sequence similarity of 96.47% (Fig. 3), indicating that they are structurally and functionally identical.

#### 3.2. Homology modeling

Since an experimentally determined structure for the TyS protein is not available, the 3D structure was predicted and constructed using the Schrodinger suite's homology modeling panel. With a 96.47% identity percentage, the *L. major* protein (PDB ID: 2VOB) was chosen as the template sequence. Following model prediction, the Ramachandran plot was used for modelled protein validation. This

**Table 1**  
Docking score and 2d-interaction of top three compounds against TyS protein by using virtual screening.

Ligand ID	Compound Name	Docking score (kcal/mol)	Hydrogen bond interaction	Pi-pi stacking	Pi-cation interaction
ZINC000003800008	Dostinex	-11.927	Ser230, Phe626		Phe626
ZINC000000538275	Raloxifene	-10.568	Ser230, Phe249, Ala628, Ser264	Phe626, Trp363	
ZINC000000000856	Formoterol	-10.446	Trp363, Met251, Gly250, Phe626	Phe626	Trp363, Phe626

**Table 2**  
Binding free energy for the top three compounds against TyS protein.

Compound Name	$\Delta G_{bind}$	$\Delta G_{covalent}$	$\Delta G_{coulomb}$	$\Delta H_{bond}$	$\Delta G_{lipo}$	$\Delta G_{vdw}$
Dostinex	-56.21	3.79	-103.85	-1.01	-18.30	-51.61
Raloxifene	-70.41	3.80	-77.28	-2.12	-32.52	-43.21
Formoterol	-64.15	4.76	-70.26	-2.66	-22.70	-38.65

**Table 3**  
Physicochemical & Pharmacokinetic parameter of top three compounds by using qikprop of Schrodinger suite.

Compound Name	Molecular wt.	Donor Hb	Acceptor Hb	QPlogS	QPlogO/W	oral human Absorption	QPPCaCo	QPlogBB
Dostinex	451.611	1	6.5	-4.504	4.137	3	78.235	0.008
Raloxifene	473.586	2	6.25	-6.48	4.86	1	118.857	-1.027
Formoterol	344.41	4	7.2	-2.317	1.476	2	46.297	-1.402

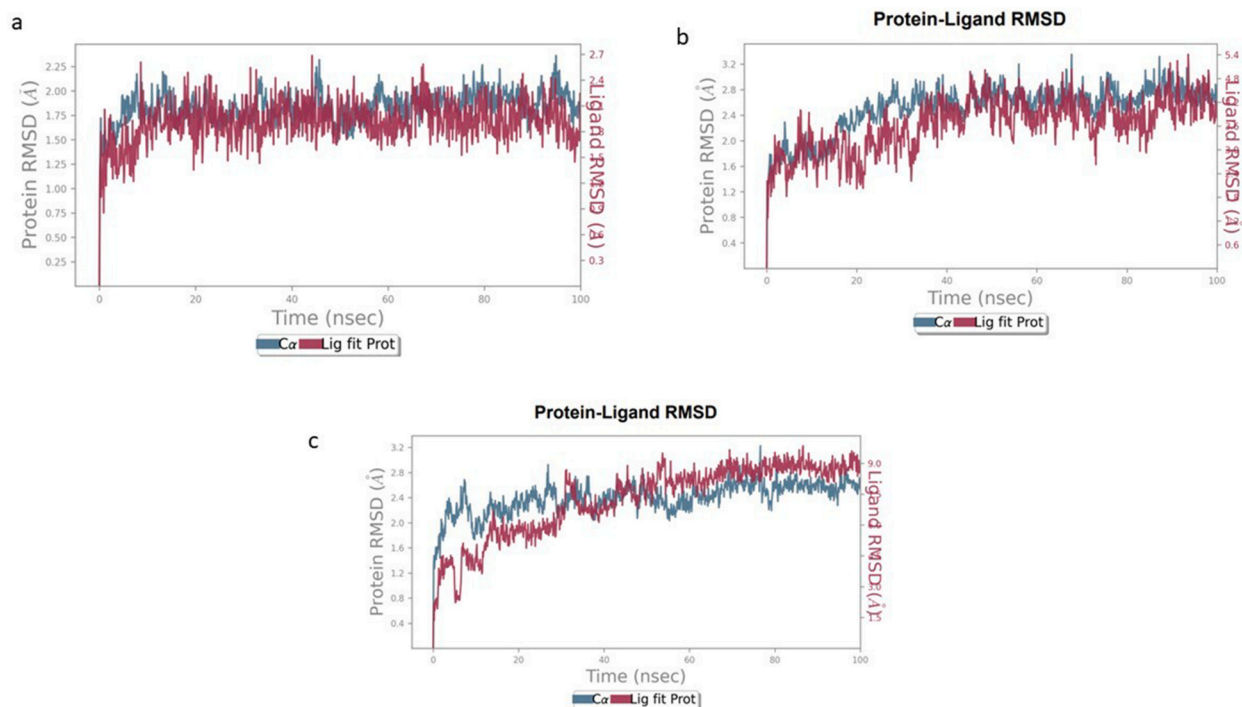


**Fig. 6.** RMSD plot of protein-ligand complex during 100 ns(ns) MD simulation. Blue line in graph shows protein RMSD in form of C alpha chain of protein and pink lines represents Lig fit Prot RMSD, protein RMSD values are on left y-axis while lig fit prot RMSD are on right Y-axis, the X-axis shows time period of MD simulation in ns (a) RMSD of Dostinex, (b) RMSD of Raloxifene and (c) RMSD of Formoterol.

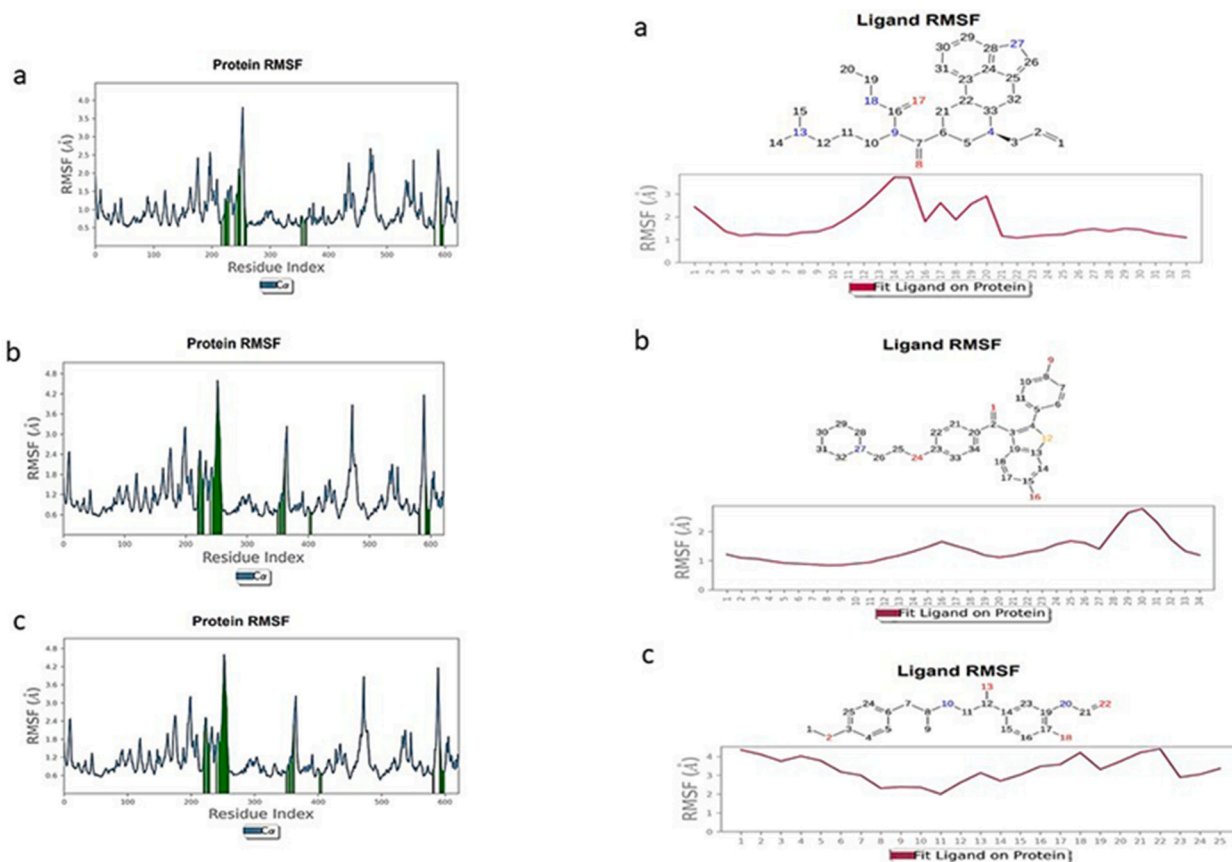


**Fig. 7.** RMSF plot of Protein-ligand complex during 100ns MD simulation. In plot the active site residues are on Y-axis and X-axis shows time period of MD simulation in nanoseconds. (a)Dostinex, (b)Raloxifene and (c)Formoterol; Ligand RMSF plots of the compounds (d) Dostinex, (e) Raloxifene and (f) Formoterol. The pink line in the plot shows RMSF of ligand atoms, the X-axis indicates residues of protein and Y-axis shows value of RMSF.

revealed that the majority of the model structures amino acids lie in the preferred region (>90%), indicating stability (Fig. 4). Furthermore, the binding site in the TyS protein was predicted using the Schrodinger software's sitemap module with a Site-Score value of 1.07.

### 3.3. Virtual screening

Structure-based virtual screening technique was used to find the drugs that could be repurposed to target the TyS protein and treat leishmaniasis. The VSW panel received the receptor grids as a receptor source, and the structures of 2000 compounds in the FDA-approved drug library were obtained in SDF format from the ZINC-15 database were used as ligands and prepared using Ligprep.

The compounds were filtered according to their physicochemical characteristics, absorption, distribution, metabolism and elimination (ADME) characteristics, and Lipinski's rule of five using QikProp to obtain drug like molecules. Further, the molecules with zero "Rule of Five" violation were subjected for molecular docking with the TyS protein which occurred sequentially using HTVS, SP, and XP modes filtering the top 10% best ligands in each step. This resulted in generation of three hits i.e., Dostinex (ZINC000003800008) with a docking score of  $-11.927$  kcal/mol, while Raloxifene (ZINC000000538275) and Formoterol (ZINC0000000008561) with  $-10.568$  kcal/mol and  $-10.446$  kcal/mol, respectively. The receptor-ligand interactions were visualized using 2D viewer. Dostinex formed two hydrogen bond interactions at Ser230 and Phe626, one salt bridge interaction with Asp252, and one pi-cation interaction with Phe626 in the active site of TyS protein (Fig. 5a). Raloxifene formed four hydrogen bond interactions with Ser230, Phe249, Ala628, and Ser264 and one pi-pi stacking interaction with Phe626 and Trp363 (Fig. 5b). The third hit, i.e., Formoterol, was found to form four hydrogen bond interactions with Trp363, Met251, Gly250, and Phe626, one pi-pi stacking interaction with Phe626, and two pi-cation interactions with Trp363 and Phe626 residues in the binding site (Fig. 5c). The hydrogen bond interactions with Ser230 and pi-pi stacking interaction with Phe626 were found to be common in the above three compounds, which can be assumed as a crucial interaction for inhibiting TyS function of *L. donovani*.

The physico-chemical properties, docking score, and interaction of top three hits were shown in Table 1 and Table 2, respectively.



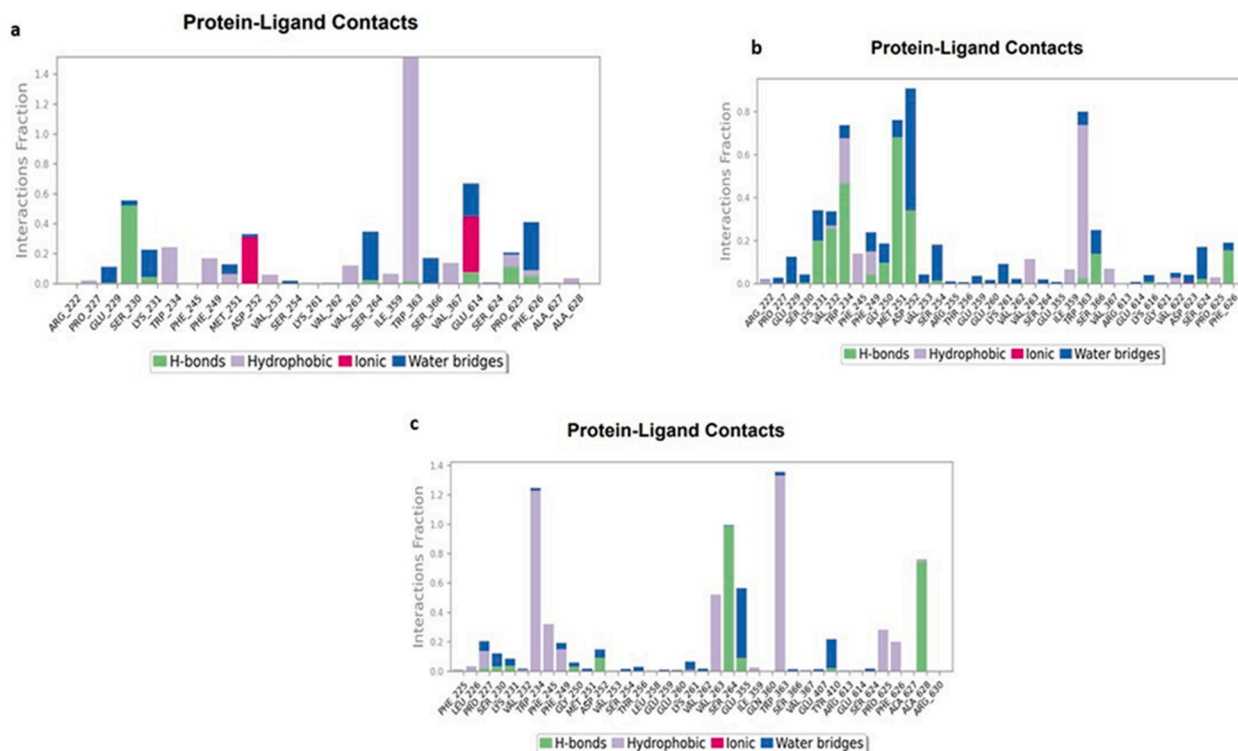


**Fig. 8.** Protein-ligand Contacts histogram shows ligand interaction with amino acids at binding site, purple for hydrophobic interaction, green for hydrogen bond, pink for ionic interaction and blue for water bridge. X-axis indicate amino acid residues while Y-axis shows Interaction fraction; (a) Dostinex, (b) Raloxifene (c) Formoterol.

### 3.4. Binding free energy analysis

The MM/GBSA approach was used to assess the docked complex's binding free energies. The results showed that the Dostinex-Tys, Raloxifene-Tys, and Formoterol-Tys complexes showed the binding energy of  $-56.21$  kcal/mol,  $-70.41$  kcal/mol, and  $-64.15$  kcal/mol, respectively. The binding free energy suggests that the lead molecules may exhibit a strong affinity towards the amino acid residues in the binding region of the target protein. The binding energy of the hit compounds is shown in [Table 3](#).

### 3.5. Molecular dynamic simulation

To investigate the movement of molecules in complex systems, 100 ns of MD simulations were run for the Dostinex, Raloxifene, and Formoterol protein complexes. This is carried out to precisely characterize the changes in conformations, energetics, and interactions between the ligand and the protein. To determine the system's overall potential energy based on the reliability of interactions between specific atom-atom pairs, a force field is used. First, RMSD and RMSF were used to examine MD trajectories in order to determine the stability as well as fluctuation of the complex structures.

#### 3.5.1. Protein and ligand RMSD

To measure the number of conformational changes in the protein-docked complex, RMSD was calculated for 100ns. In order to analyze the equilibrium of MD trajectories and assess the stability of protein-ligand complex systems during the simulation process, the root mean square deviation (RMSD) is used. It helps to measure how much distance the protein deviates from the backbone during the simulation period. The complex of TyS-Dostinex had a remarkably consistent RMSD within 100 ns of simulation time, with an RMSD of  $1.25$  Å and a modest fluctuation range between  $1.50$  and  $2.27$  Å ([Fig. 6a](#)). Similarly, in the case of the TyS-Raloxifene complex, it exhibited stability from 0 to 20ns. After that, it showed slight fluctuation up to 35ns followed by constant stability. It showed an average RMSD of  $2.4$  Å with a fluctuation between  $1.2$  and  $4.8$  Å ([Fig. 6b](#)). In comparison to Dostinex, it showed more RMSD. In the case of the Formoterol-Protein complex, it was unstable till the first 40ns. Then it showed no fluctuation till 100ns with a high RMSD range between  $0.8$  and  $9$  Å ([Fig. 6c](#)). Low RMSD results show that the complexes are very stable. Here, we can see that the Dostinex-Protein complex is more stable than the other two compounds as it has less RMSD.

#### 3.5.2. Protein and ligand RMSF

The flexibility of each residue in the ligand-protein complexes was evaluated and plotted using the root-mean-square fluctuations

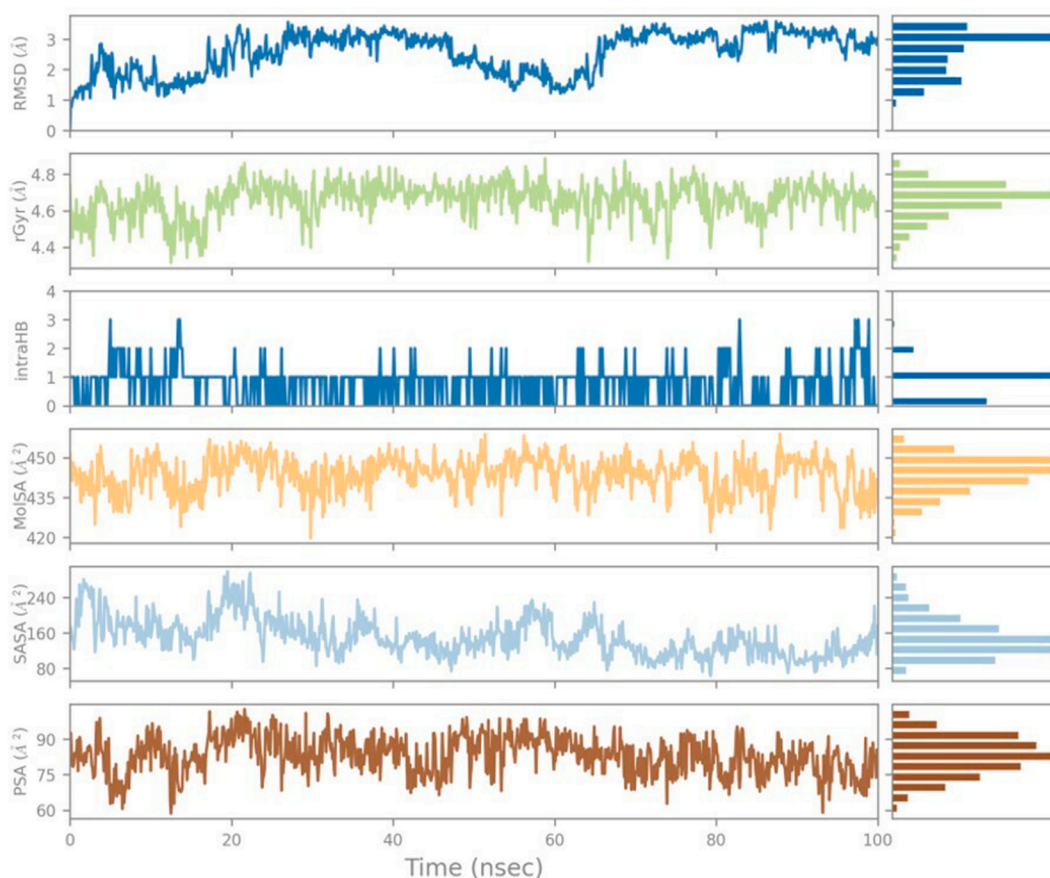


**Fig. 9.** The radius of gyration (Rg), Molecular surface area (MolSA), Solvent accessible surface area (SASA) and polar surface area (PSA) of Dostinex.

(RMSF). Greater RMSF values indicate less stability and less binding affinity of ligands, while lesser RMSF values indicate great stability and more binding affinity. The corresponding 100 ns MD trajectories were used to estimate the RMSF values. In the case of Dostinex, the protein's RMSF ranged between 0.9 and 2.0 Å (Fig. 7a). Dostinex did not show any major fluctuations in their RMSF, while element number 14 and 23 (which are not engaged in making any contact with the active site) of the Dostinex exhibited small fluctuation, which is the acceptable. Similarly, in Raloxifene, the protein's RMSF was found to be between 1.2 and 4.2 Å (Fig. 7b). The fluctuation was observed at element no.16 (pi-cation interaction), 27 (hydrogen bond interaction), and at element no.30 (not engaging in any contact with the active site). In Formoterol, the protein's RMSF was found to be 0.6–4.5 Å (Fig. 7c), but there was more variation in the ligand contact point no. 4, 6, 8, 11, 13, 14, 18, 19, 22, and 23. The result showed that Dostinex has lesser fluctuating residue comparable to the other two compounds.

### 3.5.3. Protein-ligand contacts

Key residues can engage with the binding site through non-bonding interactions, such as hydrogen bonding, which can be used to measure the binding affinity and activity of the ligand. Conformational stability may also be studied by analysing the total number of hydrogen bonds created over the simulation period. For TyS-Dostinex, H-bond was observed at Ser230 and Phe626 of protein residue (Fig. 8a). For TyS-Raloxifene, H-bond was observed at Ser230, Phe249, Ala628, and Ser264 (Fig. 8b). Similarly, for TyS-Formoterol H-bond was observed at Trp363, Met251, Gly250, and Phe626 (Fig. 8c). The common hydrogen bond interactions were observed at Ser230 and Phe626. So, these two amino acids are more crucial for binding with the protein's active site. Higher binding affinity and more stable conformation are generated by more hydrogen bonds between the ligand and the protein in the binding site.

### 3.5.4. Radius of gyration (Rg)

The structural compactness of biological macromolecules and protein-ligand complexes is measured by Rg or radius of gyration. In addition, Rg establishes the stability or instability of the protein molecule's folding depending on smaller and greater fluctuation values during the MD runtime compared to the normal. Greater Rg values indicate less stability, whereas lesser Rg values indicate more stability and compactness of the protein-ligand complex. Throughout the MD runtime, Rg values shouldn't exhibit any significant variations or fluctuations. The radius of gyration of Dostinex stayed constant during the 100 ns simulation and was found to be less than 4.8 Å (Fig. 9). It indicates that the protein- Dostinex is stable. Rg values range from 4.75 Å to 5.45 Å, with an average of 5.25 Å, for

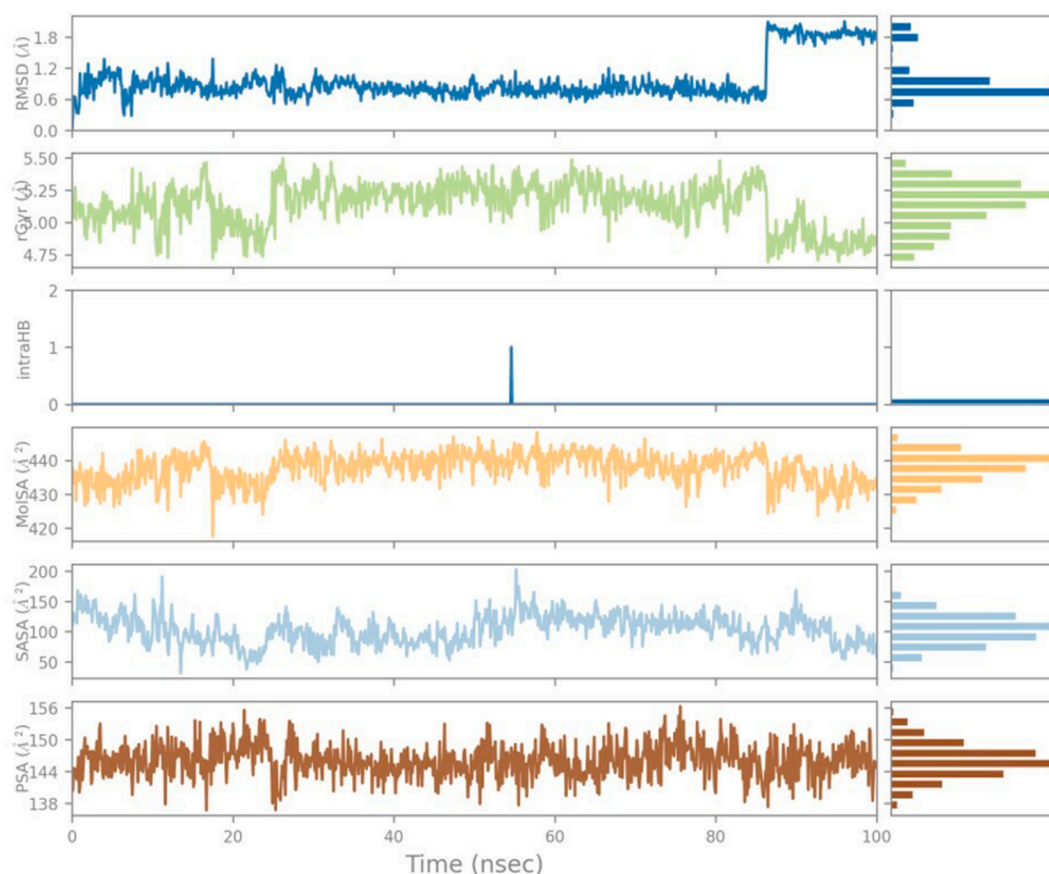


**Fig. 10.** The radius of gyration (Rg), Molecular surface area (MolSA), Solvent accessible surface area (SASA) and polar surface area (PSA) of Raloxifene.

the Raloxifene protein complex (Fig. 10). Similarly, in the case of Formoterol, the Rg was mostly in the range of 3.8–5 Å with an average of 4.5 Å (Fig. 11). So, there is no major deviation in Rg of 3 compounds.

### 3.5.5. Molecular surface area (MolSA)

MolSA is also linked to the stability of the protein-ligand complex. This value signifies van der Waals surface area. A high MolSA value indicates an unstable protein-ligand complex, whereas a lower MolSA value indicates a comparatively stable complex. Dostinex was found to be polar based on its MolSA, comparable to the van der Waals surface area, and was found to be 435–450 Å<sup>2</sup> (Fig. 9). The MolSA of Raloxifene was found to be 430–440 Å<sup>2</sup>, so it is a polar molecule (Fig. 10). The MolSA of Formoterol was found to be less than 350 Å<sup>2</sup> (Fig. 11). Here, the MolSA value was found to be stable and did not show much deviation.

### 3.5.6. Solvent-accessible surface area (SASA)

SASA, is a significant factor of MD simulation studies because it represents the surface of the protein that is accessible to the solvent molecule when it forms a strong binding with the ligand and can thus be used to anticipate the flexibility and significant conformational changes that take place during the protein-ligand interaction. Higher SASA values show more of the molecule projecting into the water, whereas lower scores show the molecule is buried within the binding site. In the case of Dostinex, SASA was found to be 160–240 Å<sup>2</sup> in the initial 20 ns. After that, it shows a range between 200 Å<sup>2</sup> in the remaining 80ns, indicating a good SASA value (Fig. 9). In the case of Raloxifene, SASA was found to be 60–150 Å<sup>2</sup>. Indicating good SASA (Fig. 10). In the case of Formoterol, SASA was found to be greater than 180 Å<sup>2</sup> initial 35ns. After that, it shows a range between 120 and 180 Å<sup>2</sup> throughout the simulation period (Fig. 11).

### 3.5.7. Polar surface area (PSA)

Polar Surface Area (PSA) is the solvent-accessible surface area in a molecule contributed only by oxygen and nitrogen atoms. PSA of Dostinex was observed between less than 90 Å<sup>2</sup> (Fig. 9). PSA of Raloxifene was found to be 140–156 Å<sup>2</sup> (Fig. 10). Formoterol was also showing a PSA of 140–165 Å<sup>2</sup> (Fig. 11). The ligands with PSA >140 Å<sup>2</sup> indicate good oral and intestinal absorption. So, Raloxifene and Formoterol may show good oral and intestinal absorption.

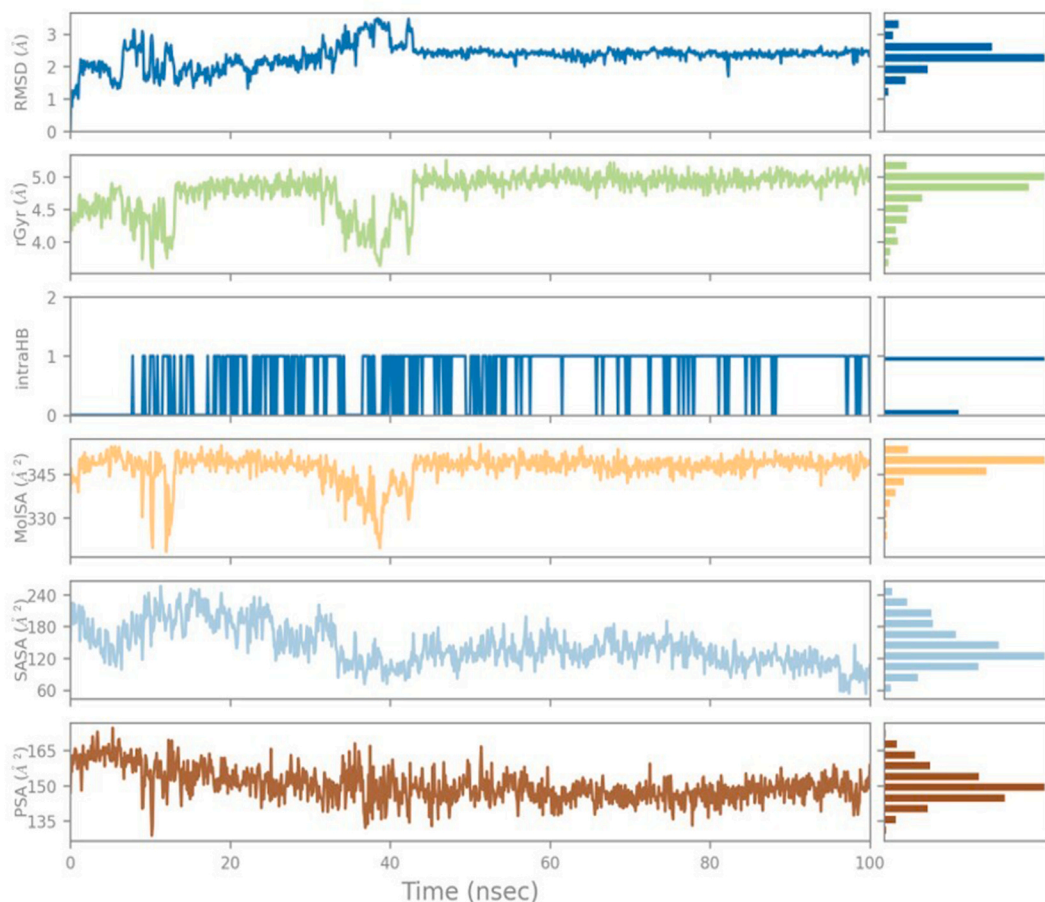


**Fig. 11.** The radius of gyration (Rg), Molecular surface area (MolSA), Solvent accessible surface area (SASA) and polar surface area (PSA) of Formoterol.

**Table 4**

Post MMGBSA of top three compounds against TyS protein.

Compound name	$\Delta G$ bind (10ns)(kcal/mol)	$\Delta G$ bind (25ns)(kcal/mol)	$\Delta G$ bind (50ns)(kcal/mol)	$\Delta G$ bind (100ns)(kcal/mol)	Mean ( $\mu$ )	Standard deviation ( $\sigma$ )
Dostinex	-80	-85	-75	-62	-75.5	9.88
Raloxifene	-91	-97	-101	-69	-89.5	14.27
Formoterol	-46.44	-46.13	-59	-56	-51.89	6.59

**Table 5**

Toxicity result of top 3 compounds by using ProTox server.

Compound name	Predicted toxicity class	Predicted LD50 dose	Toxicity end points
<b>Dostinex</b>	Toxicity class:3	200 mg/kg	Immunotoxicity, Mutagenicity
<b>Raloxifene</b>	Toxicity class:4	400 mg/kg	Immunotoxicity
<b>Formoterol</b>	Toxicity class:5	3130 mg/kg	Immunotoxicity

### 3.6. Post MM/GBSA analysis

To analyze the stability of protein-ligand complexes during the course of Molecular dynamics simulation, post-MM/GBSA calculation was done at four different time intervals-10, 25, 50, and 100 ns. This finding revealed that the dostinex-Tys protein complex have an average dGbind of  $-75.5$  and dGbind standard deviation was found to be 9.88 Whereas for raloxifene and formoterol the average dGbind was found to be  $-89.5$  and  $-51.89$  and a standard deviation of 14.27 and 6.59. The compounds raloxifene and

formoterol also showed less variation among the binding free energies of pre and post simulation period (Table 4). The free energies of the complexes at different time frames have provided comparable results with lesser deviations. As indicated by the lower binding energy values, the post MM/GBSA analysis showed that the majority of the residues in the binding site had a stable association with the compounds.

### 3.7. Toxicity prediction

Three compounds were subjected to toxicity predictions using the ProTox-II website. Dostinex was classified as toxicity class 3 and has a 200 mg/kg fatal dosage. 400 mg/kg was the lethal dose of raloxifene, which fell under toxicity class 4. A fatal dose of 3130 mg/kg was found for formoterol, which fell within toxicity class-5 (Table 5). Three substances exhibited toxicity and endpoint immunotoxicity. However, because the lethal dose is so high, these compounds are comparatively harmless.

## 4. Conclusion

In order to develop anti-leishmanial drugs, we focused on the TyS enzyme which is essential for parasite survival in stress conditions. Our computational approach; virtual screening of the FDA-approved drug library from Zinc-15 database against TyS protein has identified top-3 hits i.e., Dostinex, Raloxifene, and Formoterol. As these three compounds are FDA-approved, they have often undergone multiple phases of clinical trials before being approved. Dostinex, Raloxifene, and Formoterol have pharmacological actions that address hyperprolactinemia, regulation of the oestrogen receptor, and bronchodilator in asthma and chronic obstructive pulmonary disease (COPD), respectively. The three compounds have the potential to be druggable molecules because of their affinity and stability characteristics, which selectively block the TyS protein. These results provide a fresh avenue of inquiry for preclinical evaluation of the identified drugs chemotherapeutic potential and *in vivo* modelling.

### Data availability

The authors confirm that the data supporting the findings of this study are available within the article. Raw data that support the findings of this study are available from the corresponding author, upon reasonable request.

### Funding

The authors declare that no funds, grants, or other support were received during the preparation of this manuscript.

### CRedit authorship contribution statement

**Divya Vemula:** Writing – review & editing, Writing – original draft, Validation, Methodology, Investigation, Data curation, Conceptualization. **Shreelekha Mohanty:** Writing – original draft, Data curation. **Vasundhra Bhandari:** Validation, Supervision, Formal analysis, Conceptualization.

### Declaration of competing interest

The authors declare that they have no known competing financial interests or personal relationships that could have appeared to influence the work reported in this paper.

### Acknowledgements

The authors wish to thank the National Institute of Pharmaceutical Education and Research (NIPER) Hyderabad for the infrastructure and overall support and for software availability.

### References

- [1] S. Jain, U. Sahu, A. Kumar, P. Khare, Metabolic pathways of Leishmania parasite: source of pertinent drug targets and potent drug candidates, *Pharmaceutics* 14 (8) (2022) 1590.
- [2] F. Pasha, S. Saleem, T. Nazir, J. Tariq, K. Qureshi, Visceral leishmaniasis (Kala-Azar): a triumph against a trickster disease, *Cureus* 14 (6) (2022).
- [3] L. Abdellahi, F. Iraj, A. Mahmoudabadi, S.H. Hejazi, Vaccination in leishmaniasis: a review article, *IBJ* 26 (1) (2022), <https://doi.org/10.52547/ibj.26.1.35>.
- [4] R. Sivayogana, A. Krishnakumar, S. Kumaravel, R. Rajesh, P. Ravikanth, Treatment of leishmaniasis, *Leishmaniasis: General Aspects of a Stigmatized Disease* 67 (2022).
- [5] S. Vijayakumar, P. Das, Recent progress in drug targets and inhibitors towards combating leishmaniasis, *Acta Trop.* 181 (2018) 95–104.
- [6] M.D. Piñeyro, D. Arias, A. Parodi-Talice, S. Guerrero, C. Robello, Trypanothione metabolism as drug target for trypanosomatids, *Curr. Pharmaceut. Des.* 27 (15) (2021) 1834–1846.
- [7] B. Chawla, R. Madhubala, Drug targets in Leishmania, *J. Parasit. Dis.* 34 (2010) 1–13, <https://doi.org/10.1007/s12639-010-0006-3>.
- [8] D. Benítez, J. Franco, F. Sardi, A. Leyva, R. Durán, G. Choi, G. Yang, T. Kim, N. Kim, J. Heo, K. Kim, Drug-like molecules with anti-trypanothione synthetase activity identified by high throughput screening, *J. Enzym. Inhib. Med. Chem.* 37 (1) (2022) 912–929.
- [9] A. Equbal, S.S. Suman, S. Anwar, K.P. Singh, A. Zaidi, A.H. Sardar, P. Das, V. Ali, Stage-dependent expression and up-regulation of trypanothione synthetase in amphotericin B resistant Leishmania donovani, *PLoS One* 9 (6) (2014) 97600, <https://doi.org/10.1371/journal.pone.0097600>.

- [10] Toward new antileishmanial compounds: molecular targets for leishmaniasis treatment. In *Leishmaniasis-General Aspects of a Stigmatized Disease*. IntechOpen.
- [11] M. Aamir, V.K. Singh, M.K. Dubey, M. Meena, S.P. Kashyap, S.K. Katari, R.S. Upadhyay, A. Umamaheswari, S. Singh, In silico prediction, characterization, molecular docking, and dynamic studies on fungal SDRs as novel targets for searching potential fungicides against *Fusarium wilt* in tomato, *Front. Pharmacol.* 1038 (2018), <https://doi.org/10.3389/fphar.2018.01038>.
- [12] J. Kashyap, D. Datta, Drug repurposing for SARS-CoV-2: a high-throughput molecular docking, molecular dynamics, machine learning, and DFT study, *J. Math. Sci.* 57 (23) (2022) 10780–10802.
- [13] S. Podduturi, D. Vemula, S. Singothu, V. Bhandari, In-silico investigation of E8 surface protein of the monkeypox virus to identify potential therapeutic agents, *J. Biomol. Struct. Dyn.* (2023) 1–14.
- [14] M. Johnson, I. Zaretskaya, Y. Raytselis, Y. Merezuk, S. McGinnis, T.L. Madden, NCBI BLAST: a better web interface, *Nucleic Acids Res.* 36 (suppl\_2) (2008). W5-W9.
- [15] F. Sievers, D.G. Higgins, Clustal Omega for making accurate alignments of many protein sequences, *Protein Sci.* 27 (1) (2018) 135–145.
- [16] J.J. Sahayarayan, K.S. Rajan, R. Vidhyavathi, M. Nachiappan, D. Prabhu, S. Alfarraj, S. Arokiyaraj, A.N. Daniel, In-silico protein-ligand docking studies against the estrogen protein of breast cancer using pharmacophore based virtual screening approaches, *Saudi J. Biol. Sci.* 28 (1) (2021) 400–407, <https://doi.org/10.1016/j.sjbs.2020.10.023>.
- [17] L.L.C. Schrödinger, *Schrödinger Release 2015–3: Ligprep*, Schrödinger, LLC, New York, NY, 2015.
- [18] S. Satarker, S. Maity, J. Mudgal, M. Nampoothiri, In silico screening of neurokinin receptor antagonists as a therapeutic strategy for neuroinflammation in Alzheimer's disease, *Mol. Divers.* 26 (1) (2022) 443–466, <https://doi.org/10.1007/s11030-021-10276-6>.
- [19] S. Mahmud, M.A.R. Uddin, G.K. Paul, M.S.S. Shimu, S. Islam, E. Rahman, A. Islam, M.S. Islam, M.M. Promi, T.B. Emran, M.A. Saleh, Virtual screening and molecular dynamics simulation study of plant-derived compounds to identify potential inhibitors of main protease from SARS-CoV-2. *Brief, Bioinformatics* 22 (2) (2021) 1402–1414, <https://doi.org/10.1093/bib/bbaa428>.
- [20] A.J. Owoloye, F.C. Ligali, O.A. Enejoh, A.Z. Musa, O. Aina, E.T. Idowu, K.M. Oyebola, Molecular docking, simulation and binding free energy analysis of small molecules as Pf HT1 inhibitors, *PLoS One* 17 (8) (2022) 0268269.
- [21] S. Mahmud, M.A.R. Uddin, G.K. Paul, M.S.S. Shimu, S. Islam, E. Rahman, A. Islam, M.S. Islam, M.M. Promi, T.B. Emran, M.A. Saleh, Virtual screening and molecular dynamics simulation study of plant-derived compounds to identify potential inhibitors of main protease from SARS-CoV-2. *Brief, Bioinformatics* 22 (2) (2021) 1402–1414, <https://doi.org/10.1093/bib/bbaa428>.
- [22] H.N. Banavath, O.P. Sharma, M.S. Kumar, R. Baskaran, Identification of novel tyrosine kinase inhibitors for drug resistant T315I mutant BCR-ABL: a virtual screening and molecular dynamics simulations study, *Sci. Rep.* 4 (1) (2014) 1–11, <https://doi.org/10.1038/srep06948>.
- [23] D. Vemula, D.R. Maddi, V. Bhandari, Homology modeling, virtual screening, molecular docking, and dynamics studies for discovering *Staphylococcus epidermidis* FtsZ inhibitors, *Front. Mol. Biosci.* 10 (2023) 1087676.
- [24] P. Banerjee, A.O. Eckert, A.K. Schrey, R. Preissner, ProTox-II: a webserver for the prediction of toxicity of chemicals, *Nucleic Acids Res.* 46 (W1) (2018) W257–W263.